

Model for transport of granular matter on vibratory conveyors

Hamid El hor & Stefan J. Linz

Theoretische Physik, Universität Münster, Germany

Rafał Grochowski & Peter Walzel

Mechanische Verfahrenstechnik, Universität Dortmund, Germany

Christof A. Kruelle, Mustapha Rouijaa, Andreas Götzendorfer & Ingo Rehberg

Experimentalphysik V, Universität Bayreuth, Germany

ABSTRACT: The transport of granular matter on vibratory conveyors has attracted renewed interest because novel interesting properties such as current reversal and pattern forming structures have been detected (cf. the contribution by Kruelle et al. in this volume). Here, we present a macromechanical model for the transport of granular matter on linear, horizontal conveyors subject to linear, circular or elliptic oscillations and compare it to experimental results. This model approximates the many-grain dynamics of a granular layer by the motion of a granular block treated in analogy to the bouncing and sliding dynamics of a single particle. Using a combination of a solid and a velocity-dependent friction during the sliding process, quantitative agreement with experiments can be achieved for a wide range of driving amplitudes and frequencies.

1 INTRODUCTION

Vibratory conveyors, i.e. troughs that are externally driven by a combination of vertical and horizontal oscillations, are a standard industrial device for the effective transport of granular materials. The dynamics and the global transport properties of layers of granular particles conveyed on them, however, is far from being theoretically well understood (Rademacher 1994; Sloot & Kruyt 1996). Recently, experimental studies of the transport of granular matter on *annular* vibratory conveyors subject to *circular* driving have revealed that changes of the transport direction (current reversals) and optimal transport conditions in both directions can be achieved by varying the driving frequency and/or amplitude (Grochowski et al. 2004, Rouijaa et al. 2005, Kruelle et al. 2005). Subsequently, it has been demonstrated (El hor & Linz 2005) that these properties can be understood on the basis of a macromechanical model for the global hopping and gliding dynamics of a granular block that constitutes an appropriate generalization and modification of earlier approaches for linear driving (Rademacher 1994; Sloot & Kruyt 1996). In this contribution, we give a brief account of a further generalization of this model to linear conveyors subject to three different types of forcing, i.e. linear, cir-

cular and elliptic, and to the experimentally relevant condition of constant (horizontal) mass flow. Specifically, we discuss the difference of the transport properties for the three driving modes and test the validity of the model with representative experimental data.

2 MODEL

The basic setup of the linear vibratory conveyor is schematically sketched in Fig. 1, where also the notations being subsequently used can be read off. The frame XOY is fixed in space, whereas the frame xoy is fixed to the vibratory conveyor and co-moving with it. We investigate three types of driving modes: (i) linear, (ii) circular, and (iii) elliptic. A general formula that incorporates all three types of driving is given in the fixed frame by

$$\begin{aligned} X &= A \cos \alpha \sin \omega t - B \sin \alpha \cos \omega t \\ Y &= A \sin \alpha \sin \omega t + B \cos \alpha \cos \omega t \end{aligned} \quad (1)$$

where X and Y are the coordinates of the trough, A and B the amplitudes of the trough oscillations, ω oscillation frequency of the conveyor, and α is the inclination angle of the driving with respect to the horizontal trough surface. Choosing $B = 0$ leads to a linear driving, whereas $\alpha = 0$ and $B = A$ leads to circular

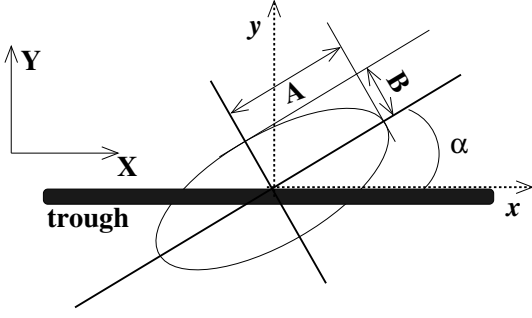


Figure 1: Sketch of the linear vibratory conveyor including its external driving.

driving. In the general case $A \neq B$ and α arbitrary, the driving is elliptic.

Our model is based on the following assumptions: (i) The moving granular material on the conveyor is effectively treated as a granular block with constant mass m that, in general, can sequentially perform two distinct types of dynamics, sliding and oblique hopping, under the action of the driving. (ii) During the sliding motion of the granular block along the trough, a dynamic friction modeled as a combination of a dry solid friction and a non-trivial lubrication-like friction is assumed. (iii) Collisions between the granular block and the trough after oblique hopping are generally inelastic. (iv) The transition from sliding to hopping happens as soon as the condition

$$\omega^2 (A \sin \alpha \sin \omega t + B \cos \alpha \cos \omega t) - g > 0, \quad (2)$$

with g being the gravitational constant, is fulfilled. As long as the upward acceleration of the conveyor is smaller than the downward gravitational acceleration, the granular block will perform a gliding motion. If Eq. 2 is fulfilled, the granular block will detach from the trough and start a free flight phase. In the following we discuss the dynamics of these two phases and the transitions between them in detail.

Gliding phase : A gliding phase takes place if, after the granular block hits the trough, the condition in Eq. 2 is not fulfilled. During this phase the granular block solely performs a sliding motion subject to friction forces and the corresponding equations of motion in the co-moving frame are determined by

$$\begin{aligned} m\ddot{x} &= \omega^2 m (A \cos \alpha \sin \omega t - B \sin \alpha \cos \omega t) + F \\ m\ddot{y} &= \omega^2 m (A \sin \alpha \sin \omega t + B \cos \alpha \cos \omega t) + N \\ &\quad - mg. \end{aligned} \quad (3)$$

Here, F represents the friction force acting on the block that combines dry solid friction and viscous-like friction and is given by

$$F = -\mu \operatorname{sgn}(\dot{x})N - m\mu_F \dot{x}, \quad (4)$$

where μ and μ_F denote the dynamic friction coefficients for solid and viscous-like friction forces, re-

spectively. Furthermore, N denotes the normal reaction force which is determined in this case by

$$N = -m\omega^2 (A \sin \alpha \sin \omega t + B \cos \alpha \cos \omega t) + mg. \quad (5)$$

Note that the dynamic friction coefficients comprise the whole complexity of the sliding behavior of the underlying interacting many-grain system and are, therefore, not directly related to the frictional behavior of a single particle. Inserting Eq. 4 and Eq. 5 in Eq. 3 yields

$$\ddot{x} + \mu_F \dot{x} = \omega^2 (A_a \sin \omega t - B_a \cos \omega t) - \mu \operatorname{sgn}(\dot{x})g \quad (6)$$

with

$$\begin{aligned} A_a &= A [\cos \alpha + \mu \operatorname{sgn}(\dot{x}) \sin \alpha] \\ B_a &= B [\sin \alpha - \mu \operatorname{sgn}(\dot{x}) \cos \alpha]. \end{aligned} \quad (7)$$

The solution for the horizontal velocity resulting from Eq. 6 reads in the case $\mu_F = 0$

$$\begin{aligned} \dot{x} &= -\omega B_a (\sin \omega t - \sin \omega t_0) \\ &\quad -\omega A_a (\cos \omega t - \cos \omega t_0) \\ &\quad -\mu \operatorname{sgn}(\dot{x})g(t - t_0) + \dot{x}_0 \end{aligned} \quad (8)$$

whereas in the case $\mu_F \neq 0$ it is given by

$$\begin{aligned} \dot{x} &= -\omega B_s [\sin \omega t - \sin \omega t_0 \chi(t, t_0)] \\ &\quad -\omega A_s [\cos \omega t - \cos \omega t_0 \chi(t, t_0)] \\ &\quad -(\mu/\mu_F) \operatorname{sgn}(\dot{x})g [1 - \chi(t, t_0)] + \dot{x}_0 \chi(t, t_0) \end{aligned} \quad (9)$$

with $\chi(t, t_0) = \exp[-\mu_F(t - t_0)]$ and

$$B_s = \frac{B_a - (\mu_F/\omega)A_a}{1 + (\mu_F/\omega)^2}, \quad A_s = \frac{A_a + (\mu_F/\omega)B_a}{1 + (\mu_F/\omega)^2}. \quad (10)$$

The index 0 denotes the initial condition at the impact and the start of the gliding phase. If the velocity changes its sign, the index 0 indicates that the solution of Eq. 3 must be reiterated with the initial condition at the time of this change. During a gliding phase, the position and the velocity of the granular block in the y-direction obviously equals zero.

Collisions with the trough: Collisions between the granular block and the trough are generally inelastic. The velocity of the granular block after the collision is given by

$$\dot{x}_i = \epsilon_t \dot{x}(t_i) \quad \text{and} \quad \dot{y}_i = -\epsilon_n \dot{y}(t_i), \quad (11)$$

where the subscript i reflects the corresponding values right at the impact. The restitution coefficients ϵ_t and ϵ_n can take arbitrary values from 0 to 1.

Free flight phase: The free flight phase starts at the lift-off time t_l determined by $\omega^2 (A \sin \alpha \sin \omega t_l + B \cos \alpha \cos \omega t_l) - g = 0$ and the

equations of motion in the co-moving frame are then given by

$$\begin{aligned} m\ddot{x} &= m\omega^2 (A \cos \alpha \sin \omega t - B \sin \alpha \cos \omega t) \\ m\ddot{y} &= m\omega^2 (A \sin \alpha \sin \omega t + B \cos \alpha \cos \omega t) - mg. \end{aligned}$$

Using the lift off initial conditions, namely $x(t_l) = x_l$, $y(t_l) = 0$, $\dot{x}(t_l) = \dot{x}_l$, $\dot{y}(t_l) = 0$, we obtain

$$\begin{aligned} \dot{x} &= -\omega B \sin \alpha (\sin \omega t - \sin \omega t_l) \\ &\quad -\omega A \cos \alpha (\cos \omega t - \cos \omega t_l) + \dot{x}_l. \end{aligned} \quad (12)$$

The subsequent impact time is determined by the next zero of the solution of the equation for $y(t)$ with the afore-mentioned initial conditions for the lift-off.

A step-by-step iteration of the combination of these dynamical phases determines the dynamics of the granular block in an algorithmic way.

3 RESULTS AND DISCUSSION

To study the transport velocity of a granular layer on a vibratory conveyor, the equations of the previous section have been numerically studied. The dynamics of the granular block has been calculated step by step during all phases when they exist. The transport velocity $\langle V \rangle$ of the granular block is defined as the mean value of the finite velocities along the trough calculated over several cycles of the conveying process, $T = 2\pi/\omega$. Looking for a reduction of the number of fit parameters, we first set the normal restitution coefficient equal to zero ($\epsilon_n = 0$), assuming by that fully plastic normal collisions of the block with the trough. We also fix the driving amplitudes A and B to the experimental values. The experiments were performed on a newly developed linear conveyor (Grochowski et al. 2004, Kruelle et al. 2005) where all three driving modes can be individually realized. In these experiments, polydisperse quartz sand with particle sizes $0.6 < d < 1.2\text{mm}$ were used and loaded with a constant throughput in range from 143 to 2860kg/(hm). Details of the experimental setup and the measurements will be given elsewhere. The remaining free model parameters are ϵ_t , μ , and μ_F . Our strategy is to start with one driving mode (the circular driving), find the fit parameters which give the best agreement with experimental data, and use them to calculate the transport velocity for the other driving modes.

(a) *Solid friction only* ($\mu_F = 0$): First we set μ_F equal to zero, i.e. assuming for the moment that the friction between the granular layer and the trough are solely described by solid friction. For circular driving, the parameters which give the best results are $\epsilon_t \approx 0.9$, and $\mu \approx 0.3$. These parameters were then used to calculate the transport velocity for linear driving with a vibrating angle $\alpha = 46.0^\circ$, and an elliptical driving with $\alpha = 30^\circ$. Fig. 2 shows the results of our calculations (crosses) in comparison to the experimental data

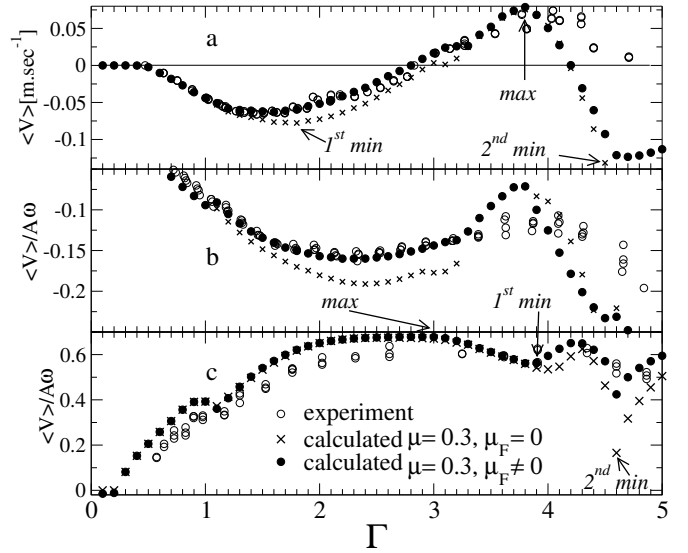


Figure 2: Comparison between the different calculated and experimental transport velocity for (a) circular, (b) elliptic, and (c) linear driving.

(open circles) as function of non-dimensionalized maximum acceleration of the trough or throw number $\Gamma = (A\omega^2/g\sqrt{B^2 + A^2 \tan^2 \alpha})[A \sin \alpha \tan \alpha + (B^2/A) \cos \alpha]$. For all three cases we find *qualitative* agreement between calculations and experiments. The calculated transport velocity reproduces the major features found in the experiments. As in the experiments, the shape of the calculated transport velocity shows the structure of maxima and minima. Moreover, the calculated transport velocity for circular driving reproduces the current reversal (as in the case of the annular conveyor (Grochowski et al. 2004, Kruelle et al. 2005)). To understand these results and the underlying dynamics of the transport velocity profile, we show in Fig. 3 the vertical motion of the trough and the granular block in the fixed frame (XOY). The motion of the granular block at the maximum of the transport velocity for the circular driving mode corresponds to a local minimum (called here first minimum) for the linear driving mode. For this specific driving acceleration, the motion of the granular block consists of successive jumps without gliding phases. On the other hand, the gliding phase is important for the minimum of the transport velocity for the circular driving mode (corresponding to a maximum of the transport velocity for the linear driving mode). There, the gliding phase coincides with a negative (respectively positive) driving acceleration of the conveyor in the x-direction for the circular (respectively linear) driving mode. The same process is repeated after two driving cycles of the conveyor leading to a second maximum and a second minimum. On the top of Fig. 3, we present a plot of the position of the different extrema (up to $\Gamma = 6$) as a function of the amplitude ratio B/A for a fixed vibration angle $\alpha = 0$. By

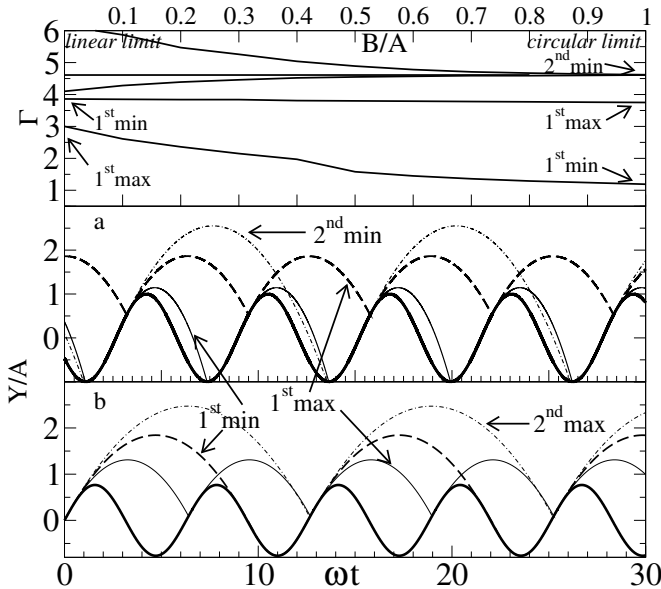


Figure 3: Representative plot of the vertical motion of the granular block at the minima and maxima of the transport velocity $\langle V \rangle$ with heavy solid lines representing the conveyor motion; (a) circular driving, (b) linear driving. On the top of the figure, we show the positions of the different maxima and minima up to $\Gamma = 6$ as function of the amplitude ratio B/A .

that, we can obtain an overview of their behavior from the linear driving limit $B/A = 0$ to the circular driving limit $B/A = 1$. Between these two limits, there is elliptic driving. At the linear limit, the number of extrema is higher and when the ratio B/A is increased, the three highest extrema converge to one limit value which is reached at the circular limit and constitutes the second minimum. The lowest extremum is the first maximum of the linear limit. The value of this extremum gradually decreases to the value of the first minimum in the circular limit. The first minimum for a linear driving gradually develops into the maximum for circular driving at roughly the same Γ -value. This figure shows that the properties of the transport velocities obtained for elliptical driving are situated in between the two extreme situations of transport velocity obtained by linear and circular driving.

An extensive study of the transport velocity where all free parameters have been systematically varied has revealed that a *quantitative* agreement between the calculated and experimental transport velocity cannot be achieved by solely invoking a solid friction force during the gliding phase.

(b) *additional velocity dependent friction*: To obtain quantitative agreement with the experimental results, an additional lubrication-type (fluid-like) friction which reflects the fluidization of the particles at the bottom seems to be reasonable. This friction takes into account that the granular matter is subject to a progressive fluidization with an increasing throw number Γ and can be modeled by a velocity-

dependent friction force: $F = m\mu_F\dot{x}$. The aspect of *progressive fluidization* is incorporated in our model via a non-constant friction coefficient $\mu_F(\Gamma)$ that has the form of $\mu_F(\Gamma) = q(\Gamma - 1)$ for $\Gamma > 1$, and $\mu_F(\Gamma) = 0$ for $\Gamma \leq 1$. Using the parameters values $\epsilon_t = 0.9$, $\mu = 0.3$, and $q = 50\text{sec}^{-1}$, we obtain a significant improvement of the agreement between the calculated and experimental transport velocities for the circular driving mode as can be seen in Fig. 2. There is good agreement between model and experimental data up to $\Gamma \approx 4.0$. Using the same fit parameters, a substantial improvement of the agreement is also obtained for linear and elliptic driving modes (see the same Figure). For throw number values $\Gamma \geq 4.0$ the agreement is not so good anymore. For such throw numbers, the granular layer becomes subject to the formation of structures with high amplitude at its surface. Then, the transport velocity is strongly influenced by the formation of these structures. Such local effects are not included in our global modeling approach.

4 CONCLUSIONS

We have presented a model for the determination of transport velocities of granular material on a vibratory conveyor subject to three different driving modes. Our calculations reproduce the major features of the transport velocity as a function of the driving, in particular the reversal of the transport direction for circular driving. Based on this model, we could explain the origin of the different behavior of the transport velocities for the different driving modes. For a *quantitative* agreement of the calculated and measured transport velocities, an additional velocity-dependent friction force during the gliding phase seems to be necessary.

This work was supported by the Deutsche Forschungsgemeinschaft (DFG-Sonderprogramm ‘Verhalten granularer Medien’).

REFERENCES

- El hor, H. & Linz, S.J. 2005. Model for transport of granular matter on an annular conveyor. *J. Stat. Mech.* Lxxx (in press).
- Grochowski, R., Walzel, P., Rouijaa, M., Kruelle, C.A. & Rehberg, I. 2004. Reversing granular flow on a vibratory conveyor. *Appl. Phys. Lett.* 84: 1019-1021.
- Kruelle, C.A., Rouijaa, M., Götzendorfer, A. & Rehberg, I., Grochowski, R., Walzel, P., El hor, H., Linz, S.J. 2005. Reversal of granular flow on a vibratory conveyor. This volume.
- Rademacher, F.J.C. & Ter Borg, L. 1994. On the theoretical and experimental conveying speed of granular solids on vibratory conveyors. *Eng. Res.* 60: 261-283.
- Rouijaa, M., Kruelle, C.A., Rehberg, I., Grochowski, R. & Walzel, P. 2005. Transport and pattern formation in granular materials on a vibratory conveyor. *Chem. Eng. Technol.* 28: 41-44.
- Slot, E.M. & Kruyt, N.P. 1996. Theoretical and experimental study of the transport of granular materials by inclined vibratory conveyors. *Powder Technol.* 87: 203-210.